THE "HEAT-PIPE" EFFECT IN VAPOR-DOMINATED GEOTHERMAL SYSTEMS

W. N. Herkelrath
U.S. Geological Survey
Water Resources Division
Menlo Park, CA 94025

Introduction

White, Muffler, and Truesdell (1971) and Truesdell and White (1973) developed a conceptual model of transport in vapor-dominated geothermal zones. The main theme of the model is that coexisting liquid and vapor phases form a counterflowing convection system similar to that observed in a heat pipe (Dunn and Reay, 1976). It is hypothesized that water evaporates from a deep water table, passes upward through the formation, and condenses at an impermeable cap rock, effectively transferring the latent heat of boiling through the formation. The liquid water then percolates downward, completing the cycle. The physics involved in the flow system is illustrated in the following analysis of an idealized one-dimensional, homogeneous, 2 km deep vapor-dominated zone which is bounded below by a water table which has a temperature of 236°C.

Flow of water and steam in the system is assumed to be described by Darcy's law for unsaturated porous materials:

$$\text{(water)} \quad q_\ell = \frac{-\rho_\ell K K_\ell}{\mu_\ell}\left(\frac{d\psi_\ell}{dZ} - \rho_\ell g\right) \qquad (1)$$

$$\text{(steam)} \quad q_v = \frac{-\rho_v K K v}{\mu_v}\left(\frac{dP_v}{dZ} - \rho_v g\right). \qquad (2)$$

The liquid water potential, ψ_ℓ, defined as the Gibb's free energy per unit volume of water, is used in place of the liquid pressure in equation (1) because flow in a highly unsaturated medium is to be considered.

Static steam zone

Consider first a static, isothermal system (zero heat flow) in which the reservoir fluids have equilibrated with the deep water table. Capillary and adsorption forces are balanced against gravity, so that the liquid water potential decreases linearly with height above the water table:

$$\psi_\ell = \rho_\ell g \left(Z - Z_o\right). \qquad (3)$$

Liquid continuity is not required for equation (3) to apply because equilibration can occur through condensation of steam.

This equation implies that two kilometers above the water table the liquid water potential is -160 bars. As is shown in figure 1, at this low potential the level of liquid saturation varies greatly from one type of porous medium to another. Water retention in the fractured porous materials which form vapor-dominated systems has not been measured. However, in order to illustrate the physical principles involved in the flow system, an estimate of the drainage characteristic has been made. For simplicity it is assumed that ψ_ℓ is uniquely related to S and T through the empirical relation

$$\psi_\ell = \psi_o (S^{-A}-1)(B-CT), \qquad (4)$$

in which ψ_o, A, B and C are constants.

Pressure in the steam phase increases with depth according to

$$P_v = P_{vo} \exp \left\{ \frac{(Z - Zo)\, Mg}{RT} \right\}. \qquad (5)$$

Equation (5) illustrates that liquid in a static vapor-dominated zone has a vapor pressure less than the saturated value. Figure 2 indicates the distribution of liquid water potential, vapor pressure, and liquid saturation in a system composed of the hypothetical material described by equation (4).

Isothermal, steady-state flow

A solution to equation (1) which is relevant to this discussion is the case of steady infiltration at the top of the steam zone. Assuming that the system is isothermal and that the water table is stationary, one can show (Childs, 1969) that the saturation decreases rapidly above the water table, but eventually assumes a constant value at which

$$KK_\ell = \frac{q_\ell \mu_\ell}{\rho_\ell^{\,2}\, g}. \qquad (6)$$

Simply stated, constant infiltration into the top of the steam zone increases the liquid saturation until the liquid permeability rises enough for the water to drain away at the same rate. Assuming an infiltration rate of 2.35×10^{-8} g/cm^2 sec, figure 3 illustrates the dependence of ψ_ℓ, P_V, and S upon depth for the hypothetical fractured material, which is assumed to have relative permeabilities given by

$$K_\ell = S^3 \qquad (7)$$

$$K_v = (1 - S). \qquad (8)$$

Nonisothermal steady-state flow

When variations in temperature are considered, the equations describing the flow can be written as

$$q_\ell = \frac{-\rho_\ell K K_\ell}{\mu_\ell} \left(\frac{\partial \psi_\ell}{\partial S} \frac{dS}{dZ} + \frac{\partial \psi_\ell}{\partial T} \frac{dT}{dZ} - \rho_\ell g \right) \quad (9)$$

$$q_v = \frac{-\rho_v K K_v}{\mu_v} \left(\frac{\partial P_v}{\partial S} \frac{dS}{dZ} + \frac{\partial P_v}{\partial T} \frac{dT}{dZ} - \rho_v g \right) \cdot \quad (10)$$

Assuming the system is closed and neglecting heat conduction

$$q_\ell = -q_v = \frac{-q_H}{L} . \quad (11)$$

equation (9), (10), and (11) may be solved to yield dT/dZ and dS/dZ as functions of temperature, saturation, the heat flow, and the properties of the medium. The distribution of T, S, ψ_ℓ, and P_v in the system can be obtained by numerical integration.

For the small gradients in temperature usually found in steam zones (Hite and Fehlberg, 1976) the extra terms in equations (9) and (10) are small and the saturation distribution is not much different from that obtained in isothermal infiltration. Liquid water condenses at the cap rock and increases the liquid saturation until the permeability becomes

$$K K_\ell = \frac{q_H \mu_\ell}{L \rho_\ell \left(\frac{\partial \psi_\ell}{\partial T} \frac{dT}{dZ} - \rho_\ell g \right)} \quad (12)$$

Assuming a heat flow rate of 4.187 x 10^{-5} j/cm^2 sec (10HFU), figure 4 illustrates the depth distribution of ψ_ℓ, P_v, and S. This heat flow results in the same condensation rate as was used in the isothermal infiltration example of figure 3.

Conclusion

Comparison of figures 2 and 4 illustrates that the liquid saturation in a two-phase convection system can be much higher than that predicted from a static pressure analysis. As a result, the "vapor pressure lowering" effect expected in a static system disappears. The decrease in P_v at the top of figure 4 is caused by temperature decrease; the relative vapor pressure in the dynamic system is above 99%.

However, the permeability used in this example is very low. At higher permeabilities the condensing steam drains out of the system much faster, and the saturation approaches the static profile.

Symbols

ℓ	- subscript indicating liquid	q_H	- heat flow rate
v	- subscript indicating vapor	R	- ideal gas constant
g	- acceleration of gravity	S	- volume relative saturation
K	- permeability	T	- absolute temperature
K_ℓ	- relative permeability	Z	- depth below caprock
M	- molecular weight of water	Z_0	- depth to water table
P_v	- vapor pressure	ρ	- density
P_{vo}	- saturation vapor pressure	μ	- viscosity
q	- mass flow rate	ψ_ℓ	- liquid water potential

REFERENCES

Childs, E. C., 1969. An Introduction to the Physical Basis of Soil Water Phenomena, Wiley (Interscience), New York.

Dunn, P. and Reay, D. A., 1976. Heat Pipes, Pergamon Press, New York.

Hite, J. R. and Fehlberg, E. L., 1976. Steam Zone Temperature Gradients at The Geysers, Summaries, Second Workshop, Geothermal Reservoir Engineering, December 1-3, Stanford University, Calif.

Truesdell, A. H. and White, D. E., 1973. Production of Superheated Steam from Vapor-Dominated Geothermal Reservoirs, Geothermics, v. 2, pp. 154-173.

White, D. E., Muffler, L. J. P., and Truesdell, A. H., 1971. Vapor-Dominated Hydrothermal Systems Compared with Hot-Water Systems, Economic Geology, v. 66, pp. 75-97.

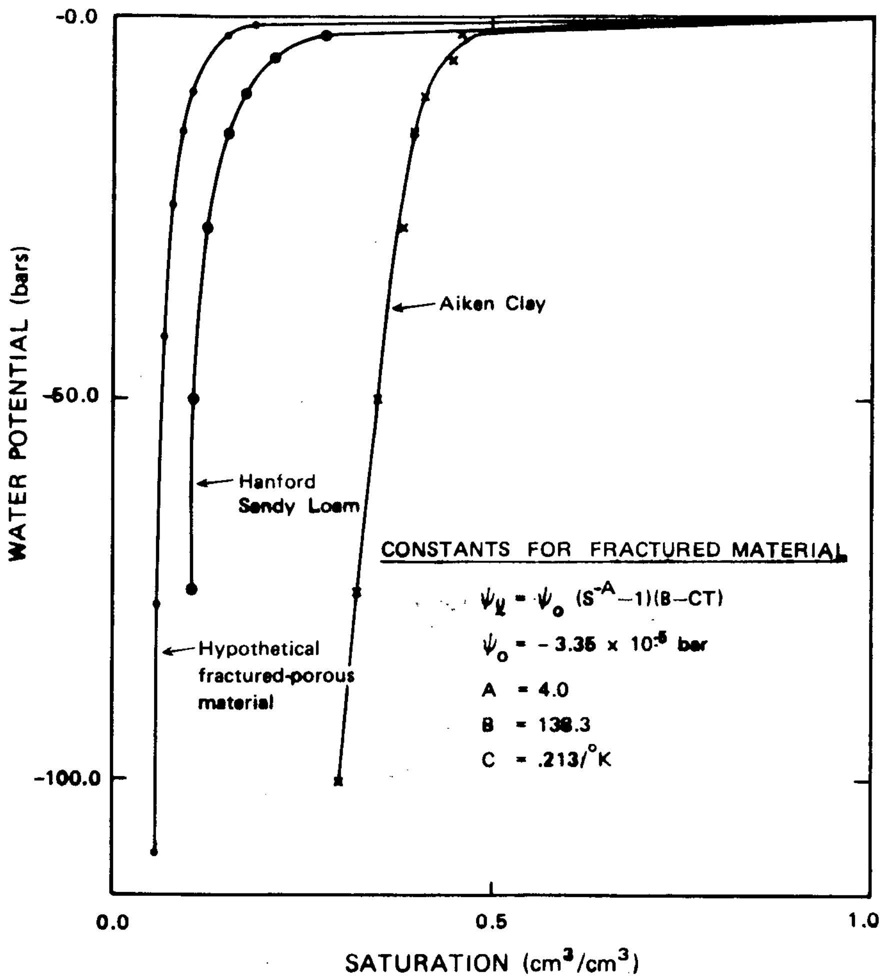

FIGURE 1. Dependence of liquid water potential upon saturation for representative porous materials.

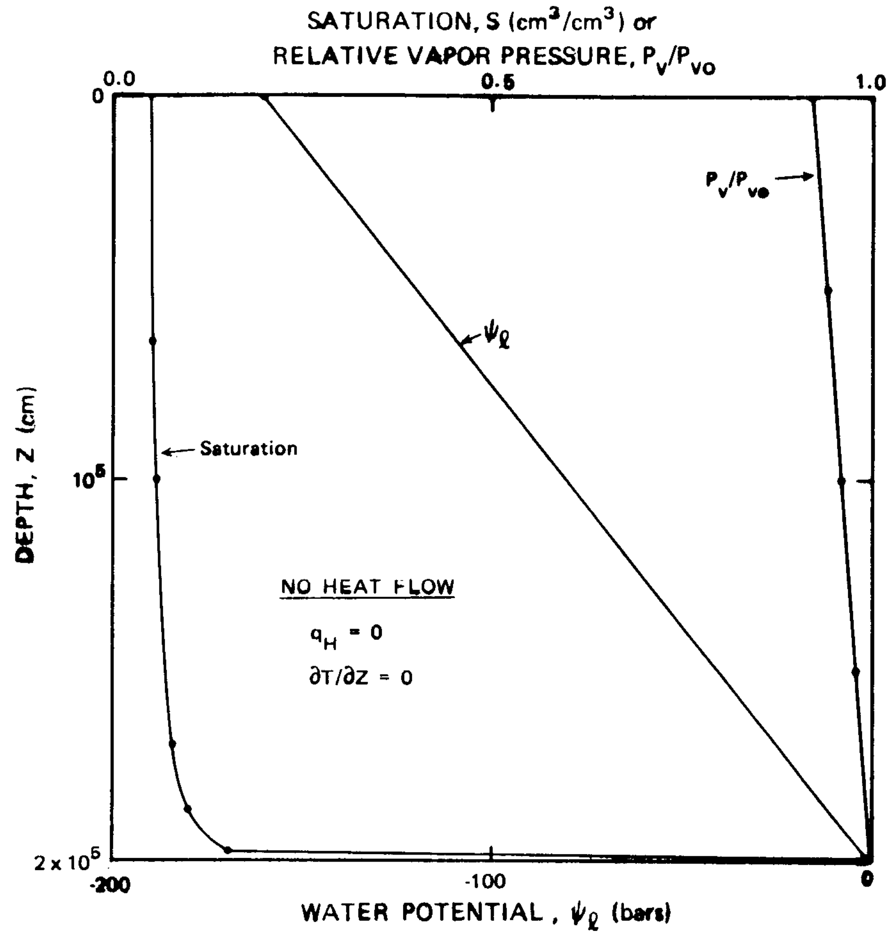

FIGURE 2. Dependence of liquid saturation, liquid water potential, and steam pressure upon depth in a static vapor-dominated zone.

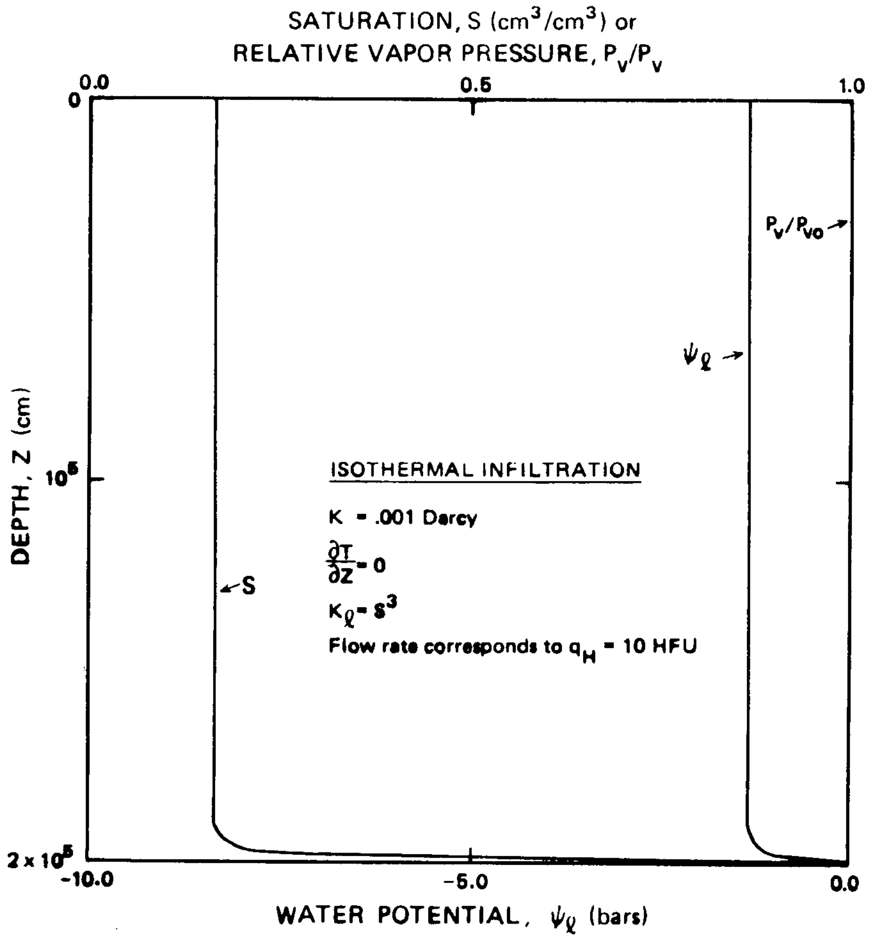

FIGURE 3. Distribution of liquid saturation, liquid water potential and steam pressure with steady isothermal infiltration of liquid at the top of a vapor-dominated zone.

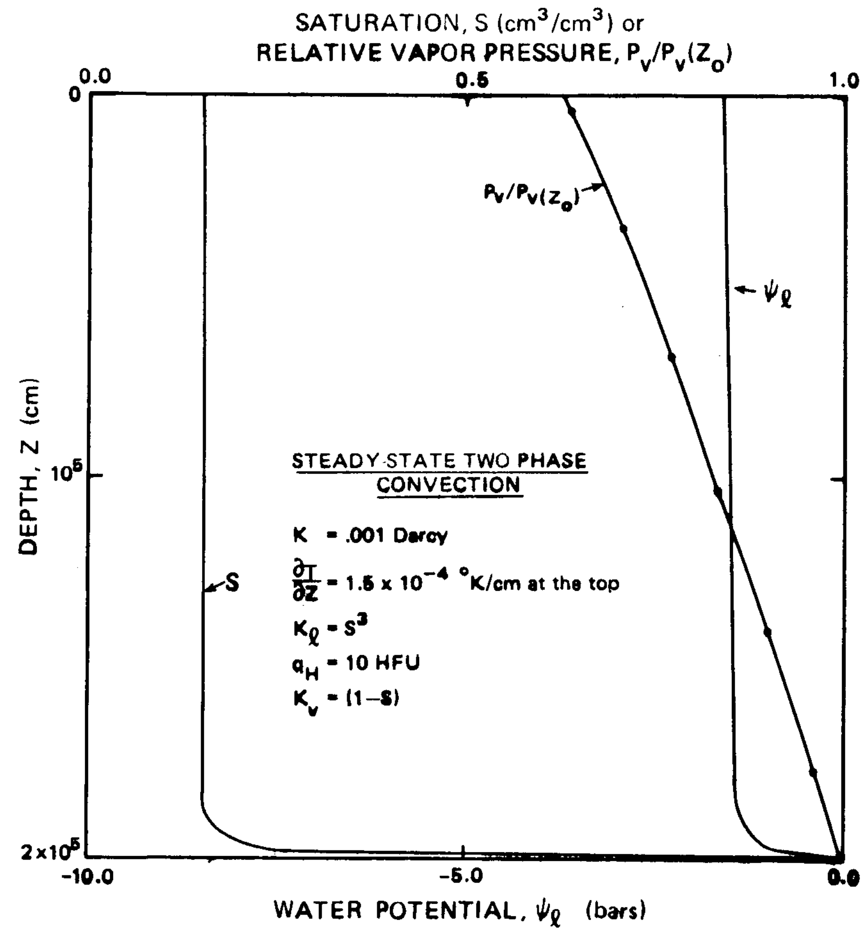

FIGURE 4. Distribution of liquid saturation, liquid water potential, and steam pressure when steam condenses at a steady rate at the top of a non-isothermal vapor-dominated zone.